



**HAL**  
open science

## Engineered borate ester conjugated protein-polymer nanoconjugates for pH-responsive drug delivery

Pei Zhou, Shuang Wu, Mohammad Hegazy, Hong Li, Xueju Xu, He Lu, Xin Huang

► **To cite this version:**

Pei Zhou, Shuang Wu, Mohammad Hegazy, Hong Li, Xueju Xu, et al.. Engineered borate ester conjugated protein-polymer nanoconjugates for pH-responsive drug delivery. *Materials Science and Engineering: C*, 2019, 104, pp.109914. 10.1016/j.msec.2019.109914 . hal-02378765

**HAL Id: hal-02378765**

**<https://normandie-univ.hal.science/hal-02378765>**

Submitted on 25 Oct 2021

**HAL** is a multi-disciplinary open access archive for the deposit and dissemination of scientific research documents, whether they are published or not. The documents may come from teaching and research institutions in France or abroad, or from public or private research centers.

L'archive ouverte pluridisciplinaire **HAL**, est destinée au dépôt et à la diffusion de documents scientifiques de niveau recherche, publiés ou non, émanant des établissements d'enseignement et de recherche français ou étrangers, des laboratoires publics ou privés.



Distributed under a Creative Commons Attribution - NonCommercial 4.0 International License

# Engineered borate ester conjugated protein-polymer nanoconjugates for pH-responsive drug delivery

Pei Zhou<sup>a,b,‡</sup>, Shuang Wu<sup>c,d,‡</sup>, Mohammad Hegazy<sup>b</sup>, Hong Li<sup>e</sup>, Xueju Xu<sup>c</sup>, He Lu<sup>d\*</sup>, Xin Huang<sup>b\*</sup>

<sup>a</sup> School of Environmental and Municipal Engineering, North China University of Water Resources and Electric Power, Zhengzhou 450011, China.

<sup>b</sup> MIIT Key Laboratory of Critical Materials Technology for New Energy Conversion and Storage, Key Laboratory of Microsystems and Microstructures Manufacturing, Ministry of Education, School of Chemistry and Chemical Engineering, Harbin Institute of Technology, Harbin 150001, China.

<sup>c</sup> The First Affiliated Hospital of Zhengzhou University, 40 Daxue Road, Zhengzhou 450052, China.

<sup>d</sup> INSERM UMR-S 1165/Université Paris Diderot, IUH, Hôpital Saint-Louis, Paris 75010, France.

<sup>e</sup> INSERM U1234/University, Faculty of Medicine and Pharmacy, Rouen, France.

Keywords: protein polymer nanoconjugates, self-assembly, borate ester bond, pH-sensitive, anti-cancer

Corresponding Authors: School of Chemistry and Chemical Engineering, Harbin Institute of Technology, China. Fax: 86-451-86403309.

E-mail: [xinhuang@hit.edu.cn](mailto:xinhuang@hit.edu.cn)

## **Abstract**

To improve the clinical efficiency of cytotoxic anticancer drugs e.g. doxorubicin (DOX), reduce the severe off-target side effects, and allow the more biocompatible and biodegradable drug penetration into tumor cells, our research efforts developed a new DOX-conjugated protein polymer nanoconjugates (PPNCs) prodrugs delivery system. Briefly, DOX was conjugated to bovine serum albumin (BSA) and the complex was treated with lactobionic acid (LA) as well as folic acid (FA) to enhance drug endocytosis and targeting selectivity. Such functionalized BSA could be conjugated with a designed phenylboronic acid functionalized poly(N-isopropylacrylamide) (PNIPAAm) *via* forming a pH-sensitive borate ester bond to give the functionalized PPNCs prodrugs. The potential of the PPNCs prodrugs on tumor cells therapy was systematically evaluated in dose/time-dependent effects. *In vitro* results showed a rapid accumulation of the prodrugs into the MDA-MB-231 tumor cell during the first 30 minutes and reached maximum at 24 hours. Moreover, the cell-killing effect was observed quickly after 4 hours incubation with an IC<sub>50</sub> of 0.5 mg/mL ( $\approx 4 \mu\text{M/L}$ ). In general, given the efficient pH-dependent DOX release of these constructed nanoconjugates, it is anticipated to contribute a potential delivery strategy for cancer therapy.

## **1. Introduction**

Cancer is a dominant intimidation to human health[1]. Toxic drugs are widely used to treat cancer, however, their side effects constitute a major obstacle in clinic. To overcome this matter, one can use prodrugs instead of drugs as a promising strategy to improve delivery of toxic effects within tumor cells greatly[2, 3]. Up to now, despite the innovation of numerous conventional drug delivery systems, the efficacy and clinical use of prodrug is still restricted by metabolism clearing mechanism, nonspecific biodistribution and multidrug resistance[4-6]. To address these restrictions, strategies toward drug delivery and delineated nanomedicine have been developed to improve the efficacy[7-10]. Such strategies widely use diverse drug delivery vehicles that are able to enhance drug penetration and detection, including liposomes[11-13], polymersomes[14-16], dendrimerosomes[17-19], inorganic particles[20-22], coacervates[23], proteinosome[24-26], and molecularly targeted nanoparticles[27, 28]. Besides, they could be used to construct drug carriers, targeted-drug delivery and nanodrugs[29-31]. In spite of these great developments, the side-effects into tissues or organs in the process of transportation, communication, metabolism and excretion, was still due to the limited biodegradability and long chronic toxic effect. Therefore, the development of novel drug delivery systems are expected to provide new

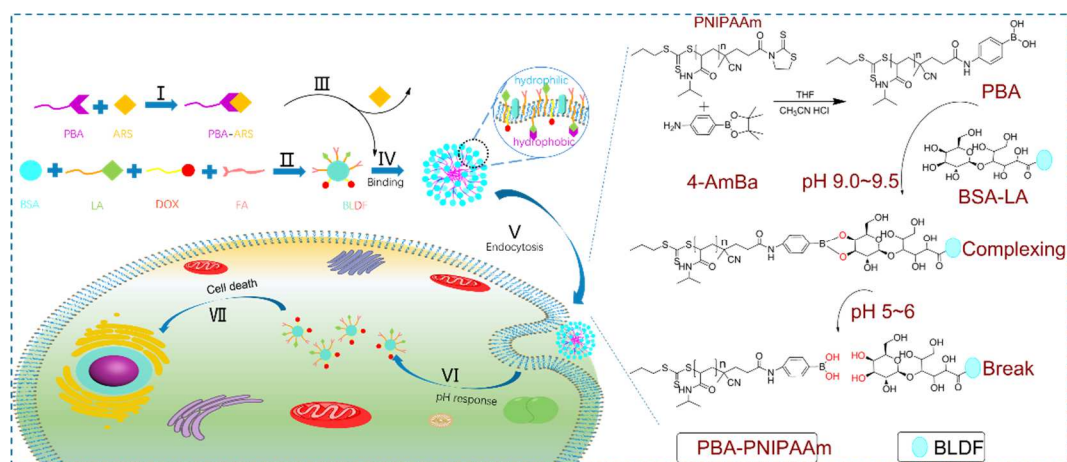
materials with improved biocompatibility and better drug payloads with selectivity, still needs our great efforts.

Recently, much attention has been paid to a new concept of directly conjugating hydrophobic drugs with good biocompatible macromolecules to form drug delivery systems. Bovine serum albumin (BSA) is a natural macromolecule endowed with many advantages for drug targeting and it is known to improve the pharmacokinetic profile of peptides, because of its good biocompatibility, facile modification, low immunogenicity, high safety and excellent biodegradability as a versatile carrier[32-34]. In comparison with other carriers, such as liposomes, polymeric micelles and inorganic particles, BSA offers the capacity of loading and delivering to the pathological sites. Additionally, folic acid (FA) has been widely employed as an active targeting agent to improve the targeting ability[35-38]. For this reason, FA has been used to deliver anticancer prodrugs because of its high binding affinity with tumor cells in liver, kidney, ovary, brain, uterus and heart[39, 40]. This effect was most likely due to FA-prodrug could be accumulated at the tumor sites, resulting in augmentation of drug uptake through folate receptor-mediated endocytosis by cancer cells[41-43]. Among these versatile nanocarriers, boronic ester conjugated with polymer was assessed as an ideal pH-responsive biomaterial to construct nanoconjugates by self-assembly, spontaneously formed a sensitive boronic ester bond in a moderate pH ( $\approx$  9-10)[44-46] and rapidly disassembled in a weak acid environment[47-53]. Thus, borate ester was

well explored in sugar sensing[54, 55], protein modification[52, 56-59], and reactive oxygen/nitrogen species detecting[60-62] as well as surface immobilizing[63-65]. Importantly, borate ester derivatives have a binding affinity to monosaccharides through a dynamic reversible process. Shin and co-workers showed a binding affinity ( $K_{eq} \approx 17800 \text{ M}^{-1}$ ) of a phenylboronic acid-salicylhydroxamic acid conjugation system[66]. As the coupling of borate ester derivatives with biological diols showed a considerable number of properties such as high stability, fast rates, potential reversibility and high pH sensitivity, it represents an additional asset when targets the cancer surface. These properties advocate considerably the merits of borate ester derivatives in modification of biocarriers in order to achieve surface immobilization along with reversible repair.

In an attempt to develop a new drug delivery system with favorable biocompatibility, high drug payloads, cancer targeted properties, effective releasing as well as multiple functionalization, we explored a novel multifunctional pH-sensitive borate ester bridging protein polymer strategy based on biocompatible and biodegradable DOX-conjugated prodrug with FA modified surface (Scheme 1, left). In the experiments, DOX was conjugated onto BSA and treated with lactobionic acid (LA) and folic acid, then reacted with phenylboronic acid (PBA) functionalized thermosensitive polymer (PNIPAAm). The resultant products were used to generate a stable pH-sensitive borate ester bridging protein polymer nanoconjugates via a covalent coupling reaction under weak alkaline conditions. Biological and

pharmaceutical properties of the final product as an anticancer agent *in vitro* were discussed.



**Scheme 1.** Schematic design of PPNCs: (left) pH-sensitive borate ester bridged BSA and PNIPAAm nanoconjugated drug-delivery system, whereas (right) formation and mechanism of protein polymer nanoconjugates (PPNCs) prodrug.

## 2. Experimental section

### 2.1 Synthesis of end-capped mercaptothiazoline-activated PNIPAAm by RAFT polymerization

The modification of mercaptothiazoline-activated PNIPAAm was prepared according to the previously reported method [67-70]. Briefly, mercaptothiazoline-activated trithiol-RAFT agent (18.9 mg, 50  $\mu$ mol), AIBN (1.7 mg, 10  $\mu$ mol), NIPAAm (847 mg, 7.5 mmol) and acetonitrile (8 mL) were added to a 25 mL round-bottom flask. The flask was then sealed and the solution degassed via four freeze pump-thaw cycles. The polymerization was carried out at 60  $^{\circ}$ C for 8 h (conversion 45%), then purified by three times precipitation in diethyl ether/hexane (2:

1 volume ratio). The obtained polymer was characterized via  $^1\text{H}$  NMR spectroscopy in  $\text{CDCl}_3$ . The proton signal ( $\delta$ , 4.58, 3.3 ppm) from mercaptothiazoline at the end of PNIPAAm chains was clearly visible in  $^1\text{H}$  NMR spectrum. The molecular weight of the obtained PNIPAAm was determined through  $^1\text{H}$  NMR by comparing the proton integral for CH signal at  $\delta = 7-7.5$  ppm in phenylboronic acid with that of the characteristic CH signal at  $\delta = 4.01$  ppm in the repeated NIPAAm units ( $M_n$  10000 g/mol).

### *2.2 Synthesis of end-capped phenylboronic acid-activated PNIPAAm*

The conjugation of 4-aminophenylboronic acid pinacol ester and end-capped mercaptothiazoline-activated PNIPAAm was carried out in an aqueous solution (pH 8.5, sodium carbonate buffer). The synthetic process was shown in scheme 1. End-capped mercaptothiazoline-activated PNIPAAm ( $M_n$  10000  $\text{g mol}^{-1}$ , 40 mg in 10 mL of water) was added to a stirred solution of 4-aminophenylboronic acid pinacol ester (4 mg, in 10 mL of PBS buffer pH 8.5) to give polymer chains for 4-aminophenylboronic acid pinacol ester with molar ratio of 1 : 5. The mixed solution was stirred for 24 h, then the product was dialyzed to remove any unreacted 4-aminophenylboronic acid pinacol ester or salts against HEPES buffer (10 mM, pH 7) three times over 24 hours and against Milli-Q water three times over 2 days. Finally, the product phenylboronic acid end-capped PNIPAAm was lyophilized and stored at  $-20\text{ }^\circ\text{C}$ .

### *2.3 Synthesis of BSA-LA complex*

The conjugation of LA to BSA via an amide bond was performed by the N-hydroxysuccinimide activated carboxyl group of LA and the amino group of BSA. Briefly, lactobionic acid (LA, 10.74 mg, 0.03 mmol), N-hydroxysuccinimide (NHS, 3.45 mg, 0.03 mmol) and 1-(3-dimethylaminopropyl)-3-ethylcarbodiimide hydrochloride (EDC, 5.76 mg, 0.03 mmol) were dissolved together in 25 mL of PBS buffer (pH 5.0, 100 mM). The reaction was carried out in dark for 60 min to activate the carboxylic groups of LA. Then, a solution of bovine serum albumin (BSA, 100 mg in 25 mL of distilled water) was added dropwise to this stirred solution and stirred for another 24 h at room temperature in the dark, as well. After the reaction completion, the solution was purified by centrifuging to remove any precipitate, after that the supernatant was dialyzed (dialysis tubing 12-14 kDa MWCO) extensively against Milli-Q water.

#### *2.4 Synthesis of DOX-BSA-LA complex*

The conjugation of DOX to BSA-LA was via an amide bond formation in aqueous solutions. In brief, BSA-LA (100 mg), N-hydroxysuccinimide (NHS, 1.725 mg, 0.015 mmol) and 1-(3-dimethylaminopropyl)-3-ethylcarbodiimide hydrochloride (EDC, 2.88 mg, 0.015 mmol) were dissolved together in distilled water (50 mL) in the dark for 60 min to activate the carboxylic groups of BSA. The pH of the reaction mixture was immediately adjusted to 5.0 by carefully adding HCl (0.5 M). Then, a solution of doxorubicin (DOX, 8.7 mg, 0.015 mmol in 25 mL of distilled water) was added slowly to the mixed solution and stirred for a further 24 h at room temperature in the dark.

After finishing the reaction, the mixed solution was purified and separated from the free DOX through centrifugation to remove any precipitate, thereafter the supernatant was dialyzed (dialysis tubing 12–14 kDa MWCO) extensively against Milli-Q water.

### *2.5 Synthesis of Folic acid-modified LA-BSA-DOX complex (BLDF)*

Folic acid (FA) was conjugated to LA-BSA-DOX via an amide bond reaction that is similar to the reaction between the residual amino group of BSA and the abundant carboxyl group of FA. Briefly, FA (6.615 mg, 0.015 mmol), N-hydroxysuccinimide (NHS, 1.73 mg, 0.015 mmol) and 1-(3-dimethylaminopropyl)-3-ethylcarbodiimide hydrochloride (EDC, 2.88 mg, 0.015 mmol) were dissolved together in 25 mL of PBS buffer (pH 5.0, 100 mM). The solution was stirred in the dark to activate the carboxylic groups of FA. After adding the solution of LA-BSA-DOX (100 mg in 25 mL of distilled water), the mixed solution was stirred in the dark for another 24 h at 25 °C. The precipitates of solution were removed by centrifuging, then the supernatant was dialyzed (dialysistubing 12-14 kDa MWCO) twice against Milli-Q water.

### *2.6 Construction of protein polymer nanoconjugates (PPNCs)*

Phenylboronic acid-activated PNIPAAm was added dropwise to a stirred solution of BLDF (1 mg in 5 mL of PBS buffer at pH 9.3). The mixed solution was incubated for 12 h at room temperature in the dark, then purified by a millipore filter ( $\Phi$  13 mm, 0.45  $\mu$ m) to remove any precipitate. After filtration, the concentrated protein polymer

nanoconjugates were obtained.

### *2.7 Characterization of protein polymer nanoconjugates (PPNCs) prodrug*

The absorption spectrum of the synthesized building blocks was measured on a PerkinElmer spectrophotometer (Lambda 750S, USA) to determine the components of LA, DOX and FA in the PPNCs prodrug. The average particle size and size distribution of the nanoconjugates (0.2 mg mL<sup>-1</sup>, pH 7.4, 5.0 mM PBS buffer) were characterized by dynamic light scattering (DLS) with an ALV-5000/E DLS instrument (Malvern Instruments, UK) at a fixed scattering angle of 90°, after being filtered by 0.45 µm Milli-pore filters. Zeta potential studies of sample solutions (0.2 mg mL<sup>-1</sup>, pH 6.8, 5.0 mM PBS buffer) were carried out at 25 °C using a ZETASIZER Nano series instrument (Malvern Instruments, UK). Transmission electron microscopy (TEM) analysis was undertaken on a JEM-1400 using a LaB6 filament at 120 kV in bright field mode. Samples were prepared by adding one drop of nanoconjugates solution (0.1 mg mL<sup>-1</sup>) onto a 300 mesh carbon film coated copper grid and the specimens were then dried in vacuum for one day. The samples for TEM observations were prepared according to the similar procedure used for SEM. SEM images were obtained on a HITACHI UHR FE-SEM SU8000 with samples sputter-coated with 10 nm platinum. Optical and fluorescence microscopy was performed on a Leica DMI8 manual inverted fluorescence microscope at 10x, 20x, 40x and 100x magnification. CLSM images were acquired using a confocal laser scanning microscope (CLSM, Nikon-A1 system, Japan), whereas the imaging parameters were kept constant for

different groups.

### *2.8 The pH sensitivity of the prodrug*

To evaluate the pH sensitivity of the prodrug (PPNCs), *in vitro* release profiles of BLDF from the PPNCs with different ratios were determined at 25 °C in PBS buffer under different pH conditions (pH 5.5, 7.4 and 9.3). PPNCs and 1 mL of ARS solution were conducted in a shaking incubator at room temperature with PBS buffer under different pH conditions (pH 5.5, 7.4 and 9.3). At predetermined time intervals, the whole solution was removed and the amount of released prodrug BLDF was calculated by UV-vis spectrometry in comparison to a standard curve. A new absorption peak at 480 nm assigned to the generated ARS-PBA and released BLDF was measured to calculate the release efficiency as described above. All experiments were performed in triplicate.

### *2.9 Cell culture and treatment*

The MDA-MB-231 human breast cancer cells (HtB-26, atCC®) were cultured at 37 °C with 5 % of CO<sub>2</sub> in RPMI-1640 medium (Eurobio, Les Ulis, France) containing 10 % FBS, 1% L-glutamine and 0.1% antibiotics (penicillin/streptomycin). While HMEC-1 (human microvascular endothelial cells) were cultured in MCDB131 medium containing 15 % FBS, 1 % L-glutamine and 0.1 % antibiotics (penicillin/streptomycin). The cells were treated with the prodrug (PPNCs) alone or in combination with different building blocks (BSA, BSA-LA, LA- BSA-FA and

PBA-Polymer) at indicated concentrations.

### *2.10 Fluorescence microscopy imaging*

To investigate the targeting ability of the prodrug to tumor cells, MDA-MB-231 with folate receptor overexpressing were selected. The cancer cells were incubated at 37 °C in the presence of 0.5 mg/mL of prodrug. After incubation for 1 h, the cells were washed three times with PBS, then fixed by 1 % paraformaldehyde and finally the nuclei were stained with DAPI. Fluorescence images were examined and collected under a ZEISS Microscopy Imaging System (Germany).

### *2.11 Flow cytometry analysis*

In flow cytometry studies, MDA-MB-231 cells were seeded in a six-well tissue culture plate (2 mL medium) at a density of  $2.0 \times 10^5$  cells per well. After 24 h, the cells were cultured with a medium containing 0.5 mg/mL of Prodrug and after incubation for 0.5 h, 4 h, 16 h, 24 h, 48 h or 72 h, the cells were trypsinized, washed resuspended in PBS and at last subjected to flow cytometry analysis (BD FACS CATON II, USA).

### *2.12 Cellular uptake study*

Cellular uptakes of BSA, BSA-LA, LA- BSA-FA, PBA-Polymer and prodrug were quantitatively estimated by flow cytometry. To investigate the uptake along with various concentrations, MDA-MB-231 cells were treated with different

concentrations (0, 0.3125, 0.625, 1.25, 2.5 mg/mL) of diverse building blocks for 48 h. While for the uptake investigation along with various times, the same mass concentration of diverse building blocks was incubated for 0.5 h, 4 h, 16 h, 24 h, 48 h and 72 h, respectively. After incubation, the cells were trypsinized, washed and resuspended in PBS. Then, the suspended cells were filtrated and examined by flow cytometry (BD FACS CATON II, USA). The instrument was calibrated with non-treated cells (negative control) to identify viable cells.

### *2.13 In vitro cytotoxicity*

Following overnight seeding into 48-well culture plates, the cancer cells MDA-MB-231 and normal cells HMEC-1 were treated with different concentrations of prodrug (PPNCs) with or without modified DOX, thereafter incubated for 24 h, 72 h and 120 h, respectively. In addition, cells treated only with the medium were incubated at the same time as a control. At last, the cells were collected and counted with a Coulter counter (Beckman, Z2, USA) to evaluate the cytotoxicity of prodrug with or without modified DOX against cancer cells MDA and the normal cell HEMC-1.

## **3. Results and discussion**

### *3.1 Self-assembly between BLDF and Polymer-PBA*

In order to reduce the adverse effects of cytotoxic drug DOX, BSA was used as a main matrix to construct a prodrug involving favorable characteristics. Since albumin

possesses large amounts of biodegradable free amino and carboxyl groups, non-toxic, low immunogenic and extremely stable in pH range of 4-9 at 60 °C, hence, these unique advantages make it suitable for prolonging activity of fast-clearance drugs when used as a drug carrier. In this study, we showed that different functional groups could be conjugated onto the surface of BSA. These groups included doxorubicin hydrochloride (DOX), lactobionic acid (which was used for conjugating to a polymeric chain by forming pH sensitive borate ester bond in the following step) and finally folic acid (which was used for promoting endocytosis along with targeting toward cancerous cells). The successful construction of these intermediate products, that involving BSA-lactobionic acid (BL), BSA-lactobionic acid-DOX (BLD) and BSA-lactobionic acid-DOX-folic acid (BLDF) were confirmed by dynamic light scattering (DLS) measurements which showed a gradual increase in the hydrodynamic diameter of the constructed intermediate building blocks from BSA (4.8 nm) to BL (5.6 nm) then to BLD (6.5 nm) and finally to BLDF (7.6 nm) (Figure 1a), as well as a corresponding change in zeta potential values from -16 mV to -21 mV then to 8.32 mV and lastly to 12.11 mV for BSA, BL, BLD and BLDF, respectively (Figure 1b). Also, the appropriate molecular weight differences arisen by conjugating with different functional groups were shown in MALDI-TOF mass spectrum profiles (Figure 1c). Moreover, from UV-vis absorption analysis, the specific absorption peaks for the different functional units were 490 nm for DOX and 350 nm for folic acid (Figure 1d). Interestingly, from primary amine titration measurements, the content of each group related to BSA molecule was about 14 of

lactobionic acid (Figure S1), 4 of DOX (Figure S2) and 9 of folic acid (Figure S3).

These results were consistent with the study of MADI-TOF MS data.

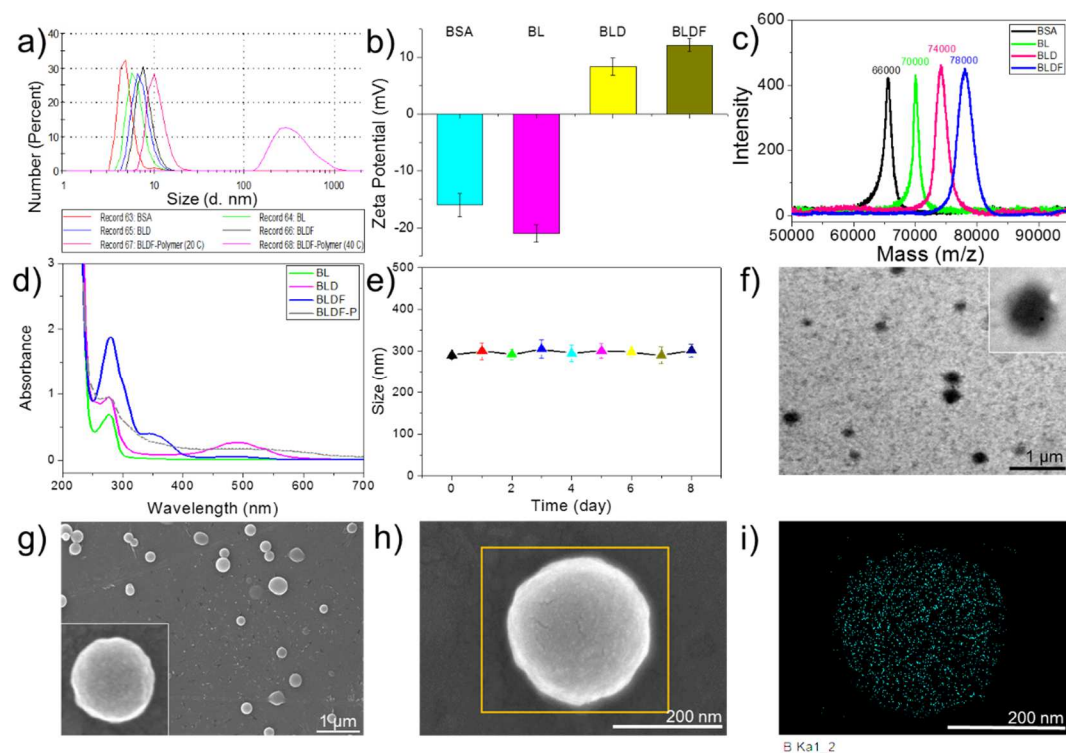


**Figure 1.** Characterization of protein polymer nanoconjugates (PPNCs) prodrug. (a,b) Hydrodynamic size distribution and zeta potential values of building blocks (0.2 mg/mL, pH=7.4) at diverse stages. (c) MALDI-TOF mass spectra of building blocks at diverse stages (BSA, BL, BLD and BLDF, respectively). (d) Normalized UV-Vis absorption spectra of diverse building blocks (BL, BLD, BLDF and BLDF-Polymer, respectively) (e) Size changes of protein polymer nanoconjugates (PPNCs) prodrug incubated in PBS (pH 9.3) containing 10 % FBS for 8 days. (f,g) TEM and SEM images for protein polymer nanoconjugates (PPNCs) prodrug, scale bars are 1  $\mu$ m. (h,i) Energy-dispersive X-ray (EDX) spectra and elemental mapping characterization of a single particle containing B element, scale bars, 200 nm.

The end-capped phenylboronic acid-functionalized poly(N-isopropylacrylamide)

(PBA-PNIPAAm) was synthesized according to a previous procedure using a well-known amide reaction between the end-capped mercaptothiazoline-activated PNIPAAm and aminophenylboronic acid.<sup>[68]</sup> As shown in Figure S4, the characteristic proton signals of phenyl group in PBA at 7.0~7.5 ppm could be discerned clearly, therefore by comparing the integration ratio between the specific signals of PBA at 7.5 ppm and those of CH group in the monomer units at 4.0 ppm, the molecular weight of PBA-PNIPAAm was estimated to be 10000 g/mol ( $M_n$ , monomer repeat units = 86). Given that the lactobionic acid involved in BLDF building blocks contains a unit of glucose and also it is a good bridging moiety, then it can allow the covalent conjugation of BLDF with boronic acid in PBA-PNIPAAm by forming a dynamic boronate ester bond. To monitor such conjugation procedure, alizarin Red S (ARS) was employed as an indicator (Figure S5), since it can bind with boronic acid to generate a blue shift on the characteristic UV-vis absorbance spectrum and a strong appeared fluorescence. As shown in Figure S6, by mixing ARS in a weak alkaline environment (pH 9.3) with PNIPAAm-PBA, there was a blue shift of 45.67 nm at wavelength of 520 nm (Figure S6a) and also a clear fluorescence emission peak at 600 nm (excitation wavelength 450 nm) (Figure S7a). By considering the strong complexation ability between lactose and PBA, thus when mixing the ARS containing PNIPAAm-PBA with BLDF, the displaced ARS resulted in a red shift of UV-vis absorbance peak besides an obvious fluorescence quenching, which well suggested the conjugation between both polymer and protein (Figure S6b, S7b). Moreover, the study of DLS at 20 °C showed that BLDF-PNIPAAm nanoconjugates gave a mean

hydrodynamic diameter of 10.12 nm, so compared with the size of BLDF (7.56 nm), it yielded an increase of ~2.56 nm which possibly is due to the presence of conjugated PNIPAAm chains (Figure 1a). In contrast, the hydrodynamic diameter of the aqueous BLDF-PNIPAAm nanoconjugates was approximately 300 nm. We attributed this large increase in the size to the aggregation of protein-polymer nanoconjugates in water. These aggregations are perhaps because of the increased hydrophobicity of hydrophobic DOX along with PBA esters, leading to their envelopment in the hydrophilic protein carrier as hydrophobic centers, thence, the self-assembly of such nanoconjugates can be occurred in the aqueous solution.

Differing from the widely reported regular amphiphilic copolymers which could self-assemble into micelle-like nanoparticles, our constructed star-like protein-polymer nanoconjugates were composed of hydrophobic DOX and PNIPAAm distributed on the surface of BSA, so they can aggregate easily into nanoparticles due to the random hydrophobic intertwining.<sup>69</sup> In this study, by using the feed molar ratio of protein to polymer (1:10) (Figure S9), and when the concentration of BLDF-PNIPAAm conjugates reached to be 0.1 mg/mL, they could aggregate into nanoparticles in the cell culture environment widely with a hydrodynamic size of 300 nm in average (DLS measurement, Figure 1e). Significantly, the formed protein-polymer nanoconjugates showed a good stability against diluting the concentration from 4 mg/mL to 0.5 mg/mL (Figure S8), as well as these nanoconjugates could keep well-dispersed in 10 % fetal bovine serum (FBS) solution without any aggregation or disassembly for over one week (Figure 1e). In general, the

formed spherical structure is clearly observed from both scanning electron microscope (SEM) and transmission electron microscopy (TEM) images (Figure 1f,g). Also, the corresponding SEM boron elemental mapping image of a single nanoparticle, whereas boron element is widely distributed inside the formed nanoparticle, suggests a random distribution of PNIPAAm during the aggregation process (Figure 1h,i). Moreover, it is worth mentioning that by varying the feed ratio of protein carrier and polymer (from 1:3 to 1:5 then 1:7), the generated protein-polymer nanoconjugates could also aggregate into nanoparticles with a size ranging from 280 nm to 330 nm with a relatively coarse surface (Figure S9). Accordingly, such constructed protein-enriched nanoparticles that composed of covalently conjugated DOX and folic acid groups onto the surface of BSA, as a favorable type of prodrug models, are expected to show good biocompatibility, high biodegradability and low side effects, which may represent a difference over other types of comparable micelles carrier models.

### *3.2 pH-dependent stability of protein polymer nanoconjugates (PPNCs)*

Given the pH sensitive boronate ester bond inside the formed nanoparticles, its dissociation under acidic environment would allow the disassembly of the protein polymer nanoconjugates. As summarized in the schematic illustration of pH-dependent dissociation for the constructed PPNCs prodrug, the dissociation in a weak acid environment and recombination in a moderate pH ( $\approx 9.0-9.5$ ) could be circulated many times (Figure 2a). The corresponding dynamic light scattering experiments showed the stable conjugated nanoparticles with negligible size changes

under a weak alkaline environment, while the size decreased seriously by transforming to a weak acid environment, suggesting the evident disassembly of nanoconjugates (Figure 2b). Such characters would allow the release of payloads from the constructed nanoparticles, especially in intracellular weak acidic environment, which is key role for antitumor efficacy. For a drug delivery system with long circulation and antitumor efficacy, it is necessary to have a high stability in the body circular system besides a fast release in the cell. To quantitatively determine the release of DOX-BSA from BSA-PNIPAAm nanoparticles, the nanoparticles were poured into a typically weak alkaline environment (pH 9.3), then in PBS buffer at pH 7.4 (corresponding to pH of blood) and finally in PBS buffer at pH 5.5 (corresponding to pH of endosome). The amount of released DOX-BSA at different predetermined time points was measured by fluorescence detector with excitation wavelength of 480 nm and emission wavelength of 580 nm. The results in Figure 2c showed that, the release efficiency of DOX-BSA from the aggregated nanoparticles was 4.95 % in the weak alkaline condition (pH 9.3) and 11.74 % in the neutral one (pH 7.4) after 48 hours. While when pH decreased to 5.5, there was an accelerated dissociation of nanoconjugates and about 50 % of DOX-BSA were released within the first 0.5 hour and 97 % were released within 4 hours. These studies well confirmed that, the constructed protein polymer nanocojugates as a novel synthesized prodrug could behave inactively during the long blood circulation, whilst they could efficiently release their targeted drug in environment of the relatively acidic cancer cells.

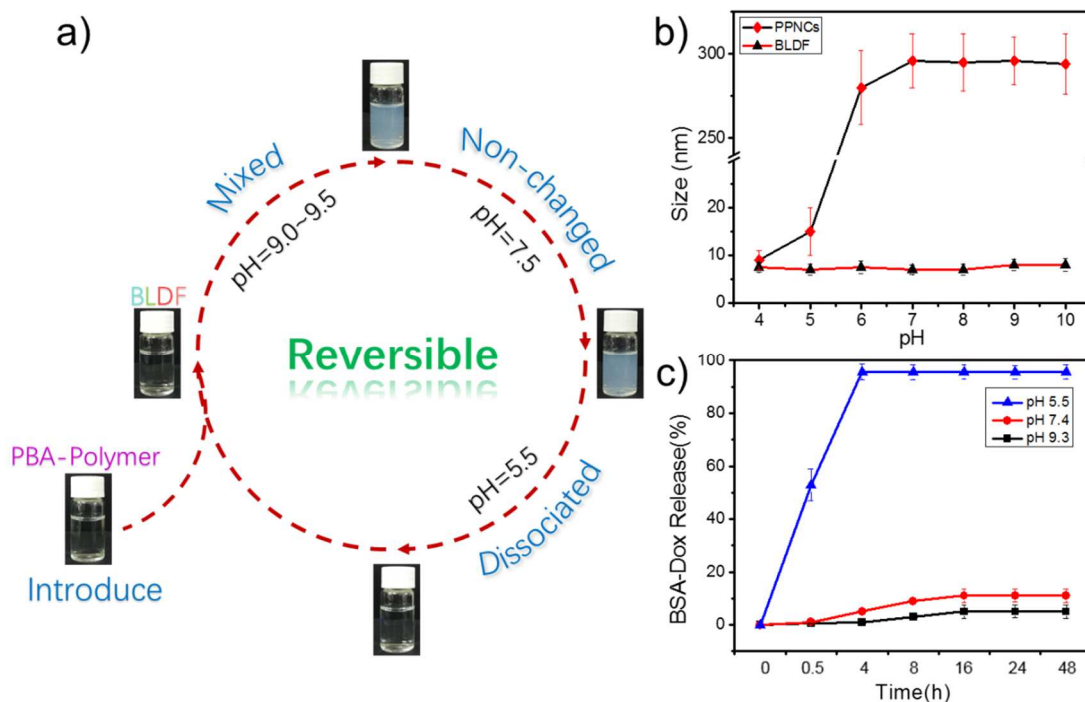


**Figure 2.** (a) Schematic illustration of pH-dependent dissociation for the constructed PPNCs prodrug, (Insets) digital photos of the functionalized protein and polymer complex in various conditions. (b) Size distribution of the prodrug (PPNCs) and the precursor protein carrier (BLDF) in different pH media ranging from 4 to 10. (c) *In vitro* pH-dependent cumulative release of BSA-DOX from PPNCs prodrug in PBS with pH values varying from 5.5, 7.4 to 9.3, respectively.

### 3.3 *In vitro* anticancer activity of protein polymer nanoconjugates prodrug

To evaluate the effect of PPNCs prodrug on tumor cells, two cell lines were used *in vitro* system: folate receptor overexpressing MDA-MB-231 cells and a low expression human normal cell HEMC-1. In this study, imaging DOX autofluorescence was evaluated by observing the distribution of PPNCs in intracellular organelles in order to determine whether PPNCs is isolated by lysosomes or lysosome-based fluorescent tracers (Lyso-Green). Consistently, Lyso-Green can label lysosomes and use

fluorescent double labeling to determine whether PPNCs is surrounded by lysosomes (by observing the overlap of PPNCs and fluorescently labeled cell vesicles) or not. The entrance of the prodrug into living cells was examined by microscopic examination as shown in Figure 3a. After 0.5 h incubation of MDA cells with PPNCs, the bright particles appeared within the cell lysosomes, indicating that nanoconjugates have been significantly endocytosed by MDA cells. The red fluorescent DOX combined nanoconjugates gave the similar result and demonstrated the quick endocytosis of the prodrug, which suggesting that the constructed nanoconjugates were easily endocytosed by MDA cells. Finally, DOX was released from nanoconjugates and accompanied by migration to lysosomes of the acidic inner environment, then it entered the nucleus gradually, which was necessary for the drug to be efficient in cancerous cells killing. The corresponding enlarged region clearly showed that the endocytic graininess nanoconjugates were gradually dissociated near the nucleus (Figure 3b).

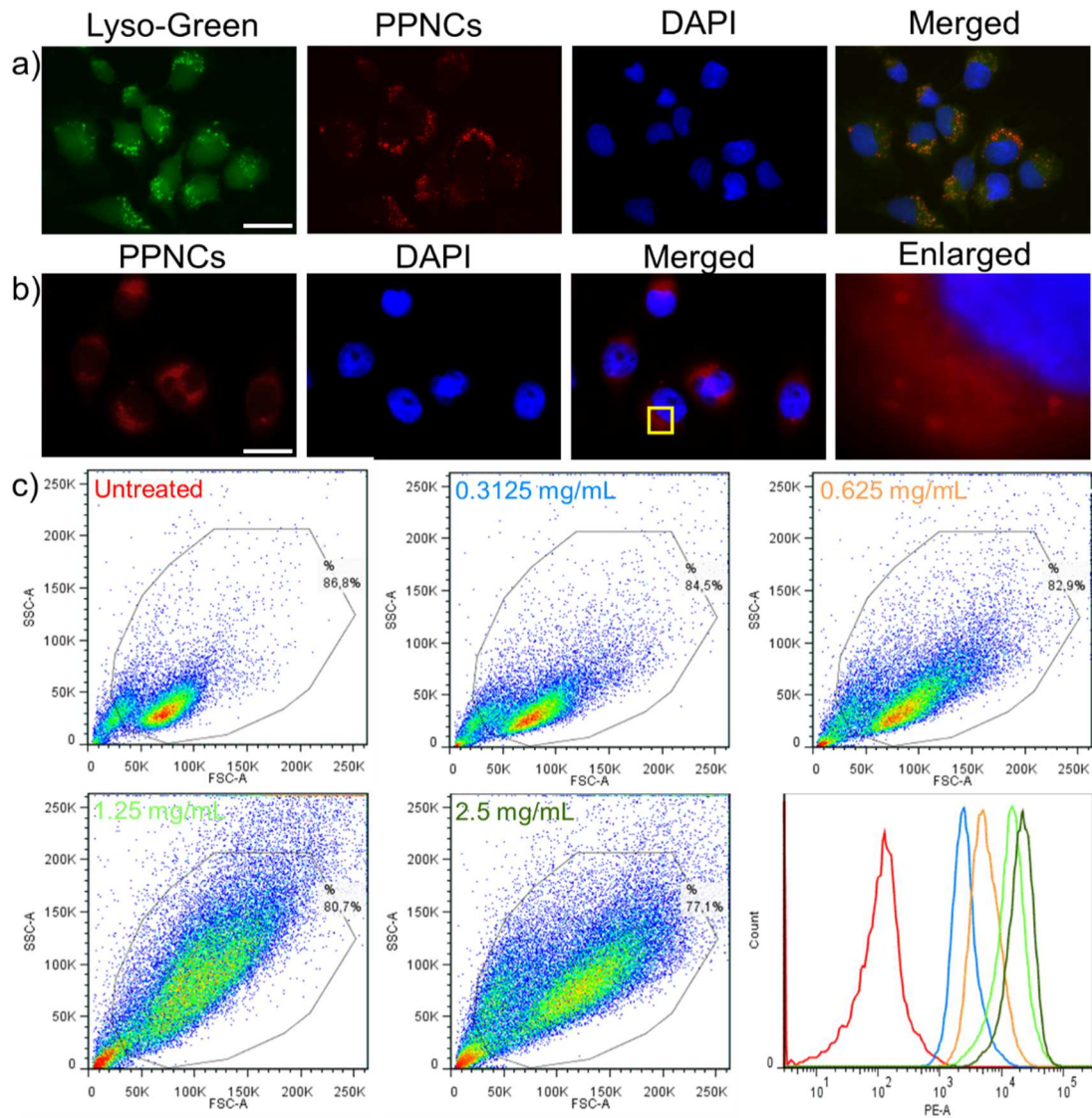


**Figure 3.** Cellular uptake of PPNCs prodrug in MDA-MB-231 cells. (a) CLSM images of MDA-MB-231 cancer cells incubated with fluorescent tracers (Lyso-Green) and PPNCs prodrug for 0.5 h. The red DOX channel and Lyso-Green labeled lysosomes were overlapped together in the merged region, scale bar, 20  $\mu\text{m}$ . (b) CLSM images of MDA-MB-231 cancer cells incubated with PPNCs prodrug for 2 h. The red area was the DOX channel, whereas the enlarged region indicated that, a gradual dissociated process was accompanied by releasing of DOX from PPNCs prodrug in the inner weak acid environment of the lysosomes, scale bar, 20  $\mu\text{m}$ . (c)

Flow cytometric profiles against MDA-MB-231 cells incubated with PPNCs prodrug in different concentration (0, 0.3125 mg/mL, 0.625 mg/mL, 1.25 mg/mL and 2.5 mg/mL, respectively).

#### *3.4 The dose-dependent effect of nanoconjugates prodrug on tumor cells*

Subsequently, flow cytometry was used to quantify endocytosis of the prodrug by cancer cells at different concentrations of nanoconjugates (Figure 3c). By increasing the concentration of nanoconjugates from 0.3125 to 2.5 mg/mL, the fluorescence of MDA had increased in a dose dependent manner, indicating that the fluorescence was accompanied by the increasing concentration of nanoconjugates. However, the nanoconjugates without DOX were also endocytosed by MDA cells with the same manner. Flow cytometry analysis also showed that, treatment of nanoconjugates with DOX induced the cell swelling, whereas the nanoaggregates without DOX were not able to collapse MDA (Figure S10). This confirms that only DOX-containing nanoconjugates can kill these cancer cells and inhibit their growth.

#### *3.5 The time-dependent effect of nanoconjugates prodrug on tumor cells*

Confocal microscopy was performed to observe the cell-killing process of nanoconjugates during first 2 hours. Nanoconjugates were gently formed small patches in the endocytosis process and most likely these patches were created in cytoplasmic macrovesicles within the first 30 minutes as shown in Figure 4a. Then, along with the accumulation of nanoconjugates in MDA for one hour, the cytoplasmic

macrovesicles fused and diffused within the MDA cells. The cytotoxic effect of nanoconjugates could be clearly observed at the end of 2 hours. Since the fluorescence was clearly dispersed in the cells, this suggesting that the disintegration of nanoconjugates was successful and started to act on the MDA cells. Actually, the accumulated nanoconjugates were between a period of 30 minutes to 2 hours within the MDA cancer cells, indicating that the uptake of nanoconjugates was time-dependent. Then, by prolonging the time of uptake, sequential analysis of the endocytosis process of MDA was carried out for 72 hours (Figure S11). In contrast to prodrug, nanoconjugates without DOX were added to MDA and the number was systematically measured by flow cytometry during 72 hours (Figure S12). The results showed a time dependent endocytosis via the endocytosis amount that rapidly reached a maximum during the first 24 hours and then stabilized during the following 48 hours. Importantly, the control experiments of nanoconjugates without DOX showed no such effect and were not able to disintegrate the cancer cells.

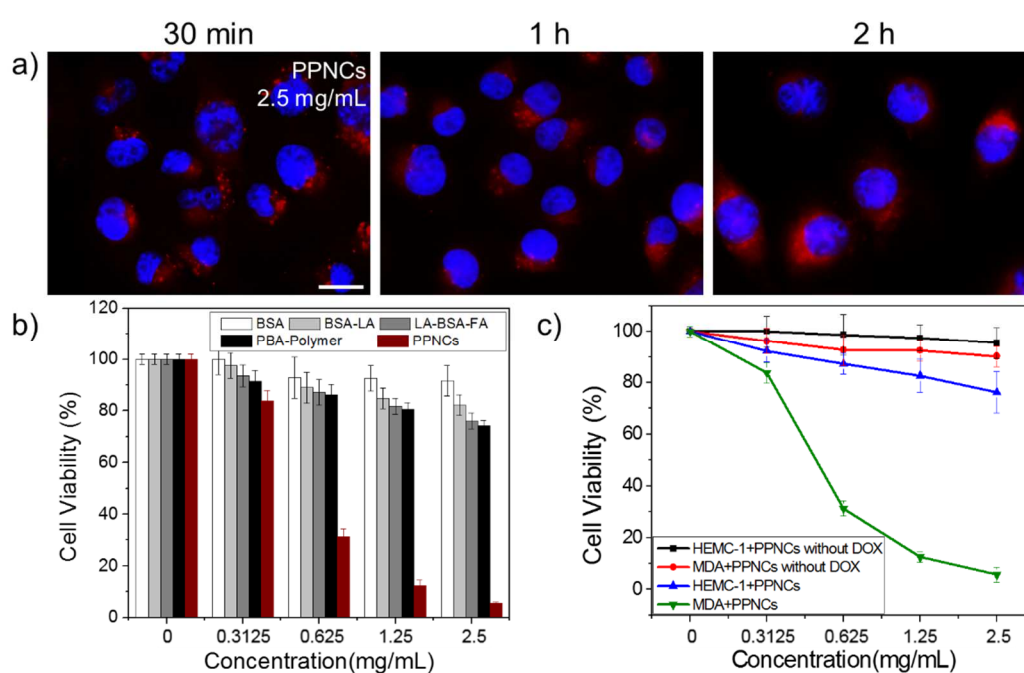


**Figure 4.** Intracellular delivery of PPNCs prodrug in MDA-MB-231 cells. (a) CLSM images of MDA-MB-231 cancer cells incubated with PPNCs (2.5 mg/mL) prodrug and their corresponding red fluorescent DOX channels after 30 min, 1 h and 2 h, scale bar, 20  $\mu$ m. (b) Relative viabilities of MDA-MB-231 cells after being incubated with various building blocks for 24 h (BSA, BSA-LA, LA-BSA-FA, PBA-Polymer and protein polymer nanoconjugates (PPNCs), respectively. (c) Cell viability was used to display the *in vitro* anticancer activity with or without modified DOX against the cancer cell MDA and the normal cell HEMC-1.

The cytotoxic effect of nanoconjugates and different building blocks was further assessed *in vitro* with cell counting method (Figure 4b). It was found that, after incubating the cells for 24 hours with different control building blocks at a concentration  $\leq 2.5$  mg/mL, over 80 % of the cancer cells survived. It indicated that the building blocks of nanoconjugates without DOX have no noticeable toxicity for MDA cells. By contrast, when the concentration of DOX-nanoconjugates reached 0.625 mg/mL, the survival rate of MDA dropped to 30 % with an IC<sub>50</sub> of about 0.5 mg/mL. When the concentration reached 2.5 mg/mL, the survival rate of MDA dropped to below 10 %, showing that nanoconjugates have a strong cytotoxic effect for MDA cells. The cytotoxicity of tumor cells was visible after 24 hours incubation and the cells growth was completely suppressed (Figure 4c). It is well known that, human blood contains albumin at a concentration of 35 - 50 g/L (3.5 - 5.0 g/dL). As albumin is a very stable protein in blood circulation and its turnover is very long (more than 24 hours), nanoconjugates after injection would be expected to circulate

and remain with a high enough concentration for achieving the therapeutic aim. Therefore, these nanoconjugates (prodrug) were suitable for carrying chemotherapeutic drugs, such as DOX in cancer therapy. Considering that the cytotoxicity of doxorubicin alone has been well characterized clinically besides its severe side effects including inhibition of human hematopoiesis and lowering in heart pumping capability, the biologic vehicles carrying such drugs are expected to protect the healthy organs and increase the therapeutic effects. Herein, we showed the generation of nanoconjugates prodrug which were able to deliver the drugs inside the cancer cells effectively, therefore, we expect this study will promote the advance in pharmaceutical technology.

#### **4. Conclusions**

In summary, an efficient approach to generate pH-sensitive protein-based nanoconjugates with size of ~300 nm was developed successfully by using protein polymer as building blocks connected together via borate ester bond. Both DOX and folic acid were incorporated onto the surface of protein covalently, and as a prodrug model, it demonstrated a lot of merits e.g. satisfactory biocompatibility, low cytotoxicity, targeted-anticancer ability as well as pH-sensitive releasing. The very low toxicity of PPNCs drug model effectively avoided the high toxicity of DOX, which is expected to not only reduce toxic side effects, but also improve anticancer efficiency *in vitro* examinations. Hence, the development of this pH-sensitive borate ester bridging protein polymer nanoconjugates model may provide a promising

strategy for practically cancer therapy and enrich the field of pharmaceutical science, especially on-demand drug-delivery systems.

### **Conflict of interest**

The authors declare no competing financial interest.

### **Author Contributions**

The manuscript was written through contributions of all authors. All authors have given approval to the final version of the manuscript.

‡These authors contributed equally.

### **Acknowledgements**

The authors acknowledge the financial support of NSFC (21474025, 21871069), the Fundamental Research Funds for the Central Universities (No.HIT.NSRIF.201830), Open Project of Key Laboratory of Microsystems and Microstructures Manufacturing (2016KM003) and the Thousand Young Talent Program for financial support.

### **References**

- [1] D. Hanahan, R.A. Weinberg, Hallmarks of cancer: the next generation, *cell*, 144 (2011) 646-674.
- [2] Z. Tang, C. He, H. Tian, J. Ding, B.S. Hsiao, B. Chu, X. Chen, Polymeric nanostructured materials for biomedical applications, *Prog. Polym. Sci.* 60 (2016) 86-128.

- [3] F. Seidi, R. Jenjob, D. Crespy, Designing smart polymer conjugates for controlled release of payloads, *Chem. Rev.* 118 (2018) 3965-4036.
- [4] E. Blanco, H. Shen, M. Ferrari, Principles of nanoparticle design for overcoming biological barriers to drug delivery, *Nat. Biotechnol.* 33 (2015) 941-945.
- [5] U. Prabhakar, H. Maeda, R.K. Jain, E.M. Sevick-Muraca, W. Zamboni, O.C. Farokhzad, S.T. Barry, A. Gabizon, P. Grodzinski, D.C. Blakey, "Challenges and key considerations of the enhanced permeability and retention effect for nanomedicine drug delivery in oncology." *Cancer Res.* 73 (2013) 2412-2417.
- [6] T.M. Allen, P.R. Cullis, Liposomal drug delivery systems: from concept to clinical applications, *Adv. Drug Delivery Rev.* 65 (2013) 36-48.
- [7] A. Maksimenko, F. Dosio, J. Mougin, A. Ferrero, S. Wack, L.H. Reddy, A.-A. Weyn, E. Lepeltier, C. Bourgaux, B. Stella, A unique squalenoylated and nonpegylated doxorubicin nanomedicine with systemic long-circulating properties and anticancer activity, *Proc. Natl. Acad. Sci. U. S. A.* 111 (2014) E217-E226.
- [8] F. Zhang, S. Zhang, S.F. Pollack, R. Li, A.M. Gonzalez, J. Fan, J. Zou, S.E. Leininger, A. Pavía-Sanders, R. Johnson, Improving paclitaxel delivery: in vitro and in vivo characterization of PEGylated polyphosphoester-based nanocarriers, *J. Am. Chem. Soc.* 137 (2015) 2056-2066.
- [9] X. Pang, Y. Jiang, Q. Xiao, A.W. Leung, H. Hua, C. Xu, pH-responsive polymer-drug conjugates: design and progress, *J. Controlled Release* 222 (2016) 116-129.
- [10] Y. Zhang, F. Huang, C. Ren, L. Yang, J. Liu, Z. Cheng, L. Chu, J. Liu, Targeted chemo-photodynamic combination platform based on the DOX prodrug nanoparticles for enhanced cancer therapy, *ACS Appl. Mater. Interfaces* 9 (2017)

13016-13028.

- [11] A.E. Hansen, A.L. Petersen, J.R. Henriksen, B. Boerresen, P. Rasmussen, D.R. Elema, P.M.a. Rosenschöld, A.T. Kristensen, A. Kjær, T.L. Andresen, Positron emission tomography based elucidation of the enhanced permeability and retention effect in dogs with cancer using copper-64 liposomes, *ACS nano* 9 (2015) 6985-6995.
- [12] X. Liu, A. Situ, Y. Kang, K.R. Villabroza, Y. Liao, C.H. Chang, T. Donahue, A.E. Nel, H. Meng, Irinotecan delivery by lipid-coated mesoporous silica nanoparticles shows improved efficacy and safety over liposomes for pancreatic cancer, *ACS nano* 10 (2016) 2702-2715.
- [13] L. Feng, M. Gao, D. Tao, Q. Chen, H. Wang, Z. Dong, M. Chen, Z. Liu, Cisplatin-prodrug-constructed liposomes as a versatile theranostic nanoplatform for bimodal imaging guided combination cancer therapy, *Adv. Funct. Mater.* 26 (2016) 2207-2217.
- [14] C.K. Wong, A.J. Laos, A.H. Soeriyadi, J. Wiedenmann, P.M. Curmi, J.J. Gooding, C.P. Marquis, M.H. Stenzel, P. Thordarson, Polymersomes prepared from thermoresponsive fluorescent protein-polymer bioconjugates: capture of and report on drug and protein payloads, *Angew. Chem., Int. Ed.* 54 (2015) 5317-5322.
- [15] J. Gaitzsch, X. Huang, B. Voit, Engineering functional polymer capsules toward smart nanoreactors, *Chem. Rev.* 116 (2015) 1053-1093.
- [16] B. Iyisan, J.r. Kluge, P. Formanek, B. Voit, D. Appelhans, Multifunctional and dual-responsive polymersomes as robust nanocontainers: design, formation by sequential post-conjugations, and pH-controlled drug release, *Chem. Mater.* 28 (2016) 1513-1525.

- [17] Q.M. Kainz, O. Reiser, Polymer-and dendrimer-coated magnetic nanoparticles as versatile supports for catalysts, scavengers, and reagents, *Acc. Chem. Res.* 47 (2014) 667-677.
- [18] T. Wei, C. Chen, J. Liu, C. Liu, P. Posocco, X. Liu, Q. Cheng, S. Huo, Z. Liang, M. Fermeglia, Anticancer drug nanomicelles formed by self-assembling amphiphilic dendrimer to combat cancer drug resistance, *Proc. Natl. Acad. Sci. U. S. A* 112 (2015) 2978-2983.
- [19] C. Hu, X. Xu, X. Zhang, Y. Li, Y. Li, Z. Gu, Bioinspired Design of Stereospecific d-Protein Nanomimics for High-Efficiency Autophagy Induction, *Chem. Mater.* 29 (2017) 7658-7662.
- [20] S.J. Soenen, W.J. Parak, J. Rejman, B. Manshian, (Intra) cellular stability of inorganic nanoparticles: effects on cytotoxicity, particle functionality, and biomedical applications, *Chem. Rev.* 115 (2015) 2109-2135.
- [21] A.C. Anselmo, S. Mitragotri, Impact of particle elasticity on particle-based drug delivery systems. *Adv. Drug Delivery Rev.* 108 (2017) 51-67.
- [22] M. Hegazy, P. Zhou, G. Wu, L. Wang, N. Rahoui, N. Taloub, X. Huang, Y. Huang, Construction of polymer coated core-shell magnetic mesoporous silica nanoparticles with triple responsive drug delivery, *Polym. Chem.* 8 (2017) 5852-5864.
- [23] C.X. Wang, S. Utech, J.D. Gopez, M.F. Mabeoone, C.J. Hawker, D. Klinger, Non-covalent microgel particles containing functional payloads: coacervation of PEG-based triblocks via microfluidics, *ACS Appl. Mater. Interfaces* 8 (2016) 16914-16921.
- [24] P. Zhou, S. Wu, X. Liu, M. Hegazy, G. Wu, X. Huang, Multifunctional and Programmable Modulated Interface Reactions on Proteinosomes. *ACS Appl.*

- Mater. Interfaces 10 (2018) 38565-38573.
- [25] X. Liu, P. Zhou, Y. Huang, M. Li, X. Huang, S. Mann, Hierarchical proteinosomes for programmed release of multiple components, *Angew. Chem. Int. Ed.* 55 (2016) 7095-7100.
- [26] Y. Zhou, J. Song, L. Wang, X. Xue, X. Liu, H. Xie, X. Huang, In situ gelation-induced death of cancer cells based on proteinosomes, *Biomacromolecules* 18 (2017) 2446-2453.
- [27] X. Li, Z. Zhou, C. C. Zhang, Y. Zheng, J. Gao, Q. Wang, Ratiometric fluorescence platform based on modified silicon quantum dots and its logic gate performance. *Inorg. Chem.* 57 (2018) 8866-8873.
- [28] X. Li, Z. Zhou, Y. Tang, C. C. Zhang, Y. Zheng, J. Gao, Q. Wang, Modulation of assembly and disassembly of a new tetraphenylethene based nanosensor for highly selective detection of hyaluronidase. *Sensor. Actuat. B-Chem.* 276 (2018) 95-100.
- [29] P. Huang, D. Wang, Y. Su, W. Huang, Y. Zhou, D. Cui, X. Zhu, D. Yan, Combination of small molecule prodrug and nanodrug delivery: amphiphilic drug-drug conjugate for cancer therapy, *J. Am. Chem. Soc.* 136 (2014) 11748-11756.
- [30] Q. Chen, C. Liang, C. Wang, Z. Liu, An imagable and photothermal “abraxane-like” nanodrug for combination cancer therapy to treat subcutaneous and metastatic breast tumors, *Adv. Mater.* 27 (2015) 903-910.
- [31] L. Qiu, T. Chen, I. Öçsoy, E. Yasun, C. Wu, G. Zhu, M. You, D. Han, J. Jiang, R. Yu, A cell-targeted, size-photocontrollable, nuclear-uptake nanodrug delivery system for drug-resistant cancer therapy, *Nano Lett.* 15 (2014) 457-463.
- [32] H. Thakkar, R.K. Sharma, A.K. Mishra, K. Chuttani, R.R. Murthy, Albumin

microspheres as carriers for the antiarthritic drug celecoxib, *AAPS PharmSciTech* 6 (2005) E65-E73.

[33]P. Zhou, L. Wang, G. Wu, Y. Zhou, M. Hegazy, X.Huang, In Situ Generation of Core-Shell Protein-Based Microcapsules with Regulated Ion Absorbance Capacity. *ChemistrySelect*, 2 (2017) 6249-6253.

[34]Z. Liu, X. Chen, Simple bioconjugate chemistry serves great clinical advances: albumin as a versatile platform for diagnosis and precision therapy, *Chem. Soc. Rev.* 45 (2016) 1432-1456.

[35]P.S. Low, S.A. Kularatne, Folate-targeted therapeutic and imaging agents for cancer, *Curr. Opin. Chem. Biol.* 13 (2009) 256-262.

[36]W. Xia, P.S. Low, Folate-targeted therapies for cancer, *J. Med. Chem.* 53 (2010) 6811-6824.

[37]C. Chen, J. Ke, X.E. Zhou, W. Yi, J.S. Brunzelle, J. Li, E.-L. Yong, H.E. Xu, K. Melcher, Structural basis for molecular recognition of folic acid by folate receptors, *Nature* 500 (2013) 486.

[38]F. Porta, G.E. Lamers, J. Morrhayim, A. Chatzopoulou, M. Schaaf, H. den Dulk, C. Backendorf, J.I. Zink, A. Kros, A. Folic acid-modified mesoporous silica nanoparticles for cellular and nuclear targeted drug delivery, *Adv. Healthcare Mater.* 2 (2013) 281-286.

[39]C.M. Paulos, M.J. Turk, G.J. Breur, P.S. Low, Folate receptor-mediated targeting of therapeutic and imaging agents to activated macrophages in rheumatoid arthritis, *Adv. Drug Delivery Rev.* 56 (2004) 1205-1217.

[40]D. Kim, E.S. Lee, K. Park, I.C. Kwon, Y.H. Bae, Doxorubicin loaded pH-sensitive micelle: antitumoral efficacy against ovarian A2780/DOX R tumor, *Pharm. Res.* 25 (2008) 2074.

- [41] Y. Chen, W. Cao, J. Zhou, B. Pidhatika, B. Xiong, L. Huang, Q. Tian, Y. Shu, W. Wen, I.-M. Hsing, Poly (L-lysine)-graft-folic acid-coupled poly (2-methyl-2-oxazoline) (PLL-g-PMOXA-c-FA): A bioactive copolymer for specific targeting to folate receptor-positive cancer cells, *ACS Appl. Mater. Interfaces* 7 (2015) 2919-2930.
- [42] P.M. Cal, R.F. Frade, V. Chudasama, C. Cordeiro, S. Caddick, P.M. Gois, Targeting cancer cells with folic acid-iminoboronate fluorescent conjugates, *Chem. Commun.* 50 (2014) 5261-5263.
- [43] Z. Wang, B. Xu, L. Zhang, J. Zhang, T. Ma, J. Zhang, X. Fu, W. Tian, Folic acid-functionalized mesoporous silica nanospheres hybridized with AIE luminogens for targeted cancer cell imaging, *Nanoscale* 5 (2013) 2065-2072.
- [44] F. Fu, Y. Wu, J. Zhu, S. Wen, M. Shen, X. Shi, Multifunctional lactobionic acid-modified dendrimers for targeted drug delivery to liver cancer cells: investigating the role played by PEG spacer, *ACS Appl. Mater. Interfaces* 6 (2014) 16416-16425.
- [45] Y. Zhao, L. Tong, Y. Li, H. Pan, W. Zhang, M. Guan, W. Li, Y. Chen, Q. Li, Z. Li, Lactose-functionalized gold nanorods for sensitive and rapid serological diagnosis of cancer, *ACS Appl. Mater. Interfaces* 8 (2016) 5813-5820.
- [46] E. Obayashi, S. Takahashi, Y. Shiro, Electronic structure of reaction intermediate of cytochrome P450<sub>nor</sub> in its nitric oxide reduction, *J. Am. Chem. Soc.* 120 (1998) 12964-12965.
- [47] Y. Zhang, Y. Guan, S. Zhou, Synthesis and volume phase transitions of glucose-sensitive microgels, *Biomacromolecules* 7 (2006) 3196-3201.
- [48] D. Roy, J.N. Cambre, B.S. Sumerlin, Sugar-responsive block copolymers by direct RAFT polymerization of unprotected boronic acid monomers, *Chem.*

Commun. (2008) 2477-2479.

- [49] J. Su, F. Chen, V.L. Cryns, P.B. Messersmith, Catechol polymers for pH-responsive, targeted drug delivery to cancer cells, *J. Am. Chem. Soc.* 133 (2011) 11850-11853.
- [50] W. Chen, Y. Cheng, B. Wang, Dual-responsive boronate crosslinked micelles for targeted drug delivery, *Angew. Chem., Int. Ed.* 51 (2012) 5293-5295.
- [51] Y. Li, W. Xiao, K. Xiao, L. Berti, J. Luo, H.P. Tseng, G. Fung, K.S. Lam, Well-defined, Reversible boronate crosslinked nanocarriers for targeted drug delivery in response to acidic pH values and cis-diols, *Angew. Chem., Int. Ed.* 124 (2012) 2918-2923.
- [52] G.A. Ellis, M.J. Palte, R.T. Raines, Boronate-mediated biologic delivery, *J. Am. Chem. Soc.* 134 (2012) 3631-3634.
- [53] J.-Y. Zhu, Q. Lei, B. Yang, H.-Z. Jia, W.-X. Qiu, X. Wang, X. Zeng, R.-X. Zhuo, J. Feng, X.-Z. Zhang, Efficient nuclear drug translocation and improved drug efficacy mediated by acidity-responsive boronate-linked dextran/cholesterol nanoassembly, *Biomaterials* 52 (2015) 281-290.
- [54] X. Wu, Z. Li, X.-X. Chen, J.S. Fossey, T.D. James, Y.-B. Jiang, Selective sensing of saccharides using simple boronic acids and their aggregates, *Chem. Soc. Rev.* 42 (2013) 8032-8048.
- [55] S. Jin, Y. Cheng, S. Reid, M. Li, B. Wang, Carbohydrate recognition by boronolactins, small molecules, and lectins, *Med. Res. Rev.* 30 (2010) 171-257.
- [56] T. Hoeg-Jensen, S. Havelund, P.K. Nielsen, J. Markussen, Reversible insulin self-assembly under carbohydrate control, *J. Am. Chem. Soc.* 127 (2005) 6158-6159.
- [57] E. Brustad, M.L. Bushey, J.W. Lee, D. Groff, W. Liu, P.G. Schultz, A genetically

- encoded boronate-containing amino acid, *Angew. Chem., Int. Ed.* 120 (2008) 8344-8347.
- [58] C.C. Liu, A.V. Mack, E.M. Brustad, J.H. Mills, D. Groff, V.V. Smider, P.G. Schultz, Evolution of proteins with genetically encoded “chemical warheads”, *J. Am. Chem. Soc.* 131 (2009) 9616-9617.
- [59] P.M. Cal, J.o.B. Vicente, E. Pires, A.V. Coelho, L.s.F. Veiros, C. Cordeiro, P.M. Gois, Boronate-mediated biologic delivery, *J. Am. Chem. Soc.* 134 (2012) 10299-10305.
- [60] A.R. Lippert, G.C. Van de Bittner, C.J. Chang, Iminoboronates: a new strategy for reversible protein modification, *J. Am. Chem. Soc.* 133 (2011) 793-804.
- [61] F. Wang, W. Niu, J. Guo, P.G. Schultz, Boronate oxidation as a bioorthogonal reaction approach for studying the chemistry of hydrogen peroxide in living systems, *Angew. Chem., Int. Ed.* 51 (2012) 10132-10135.
- [62] Z.-j. Chen, W. Ren, Q.E. Wright, H.-w. Ai, Genetically encoded fluorescent probe for the selective detection of peroxynitrite. *J. Am. Chem. Soc.* 135 (2013) 14940-14943.
- [63] H. Liu, Y. Li, K. Sun, J. Fan, P. Zhang, J. Meng, S. Wang, L. Jiang, Dual-responsive surfaces modified with phenylboronic acid-containing polymer brush to reversibly capture and release cancer cells, *J. Am. Chem. Soc.* 135 (2013) 7603-7609.
- [64] G. Pan, B. Guo, Y. Ma, W. Cui, F. He, B. Li, H. Yang, K.J. Shea, Dynamic introduction of cell adhesive factor via reversible multivalent phenylboronic acid/cis-diol polymeric complexes, *J. Am. Chem. Soc.* 136 (2014) 6203-6206.
- [65] S.D. Bull, M.G. Davidson, J.M. Van den Elsen, J.S. Fossey, A.T.A. Jenkins, Y.-B. Jiang, Y. Kubo, F. Marken, K. Sakurai, J. Zhao, Exploiting the reversible

covalent bonding of boronic acids: recognition, sensing, and assembly, *Acc. Chem. Res.* 46 (2012) 312-326.

[66] S.B.Y. Shin, R.D. Almeida, G. Gerona-Navarro, C. Bracken, S.R. Jaffrey, Assembling ligands in situ using bioorthogonal boronate ester synthesis, *Chem. Biol.* 17 (2010) 1171-1176.

[67] X. Huang, M. Li, D.C. Green, D.S. Williams, A.J. Patil, S. Mann, Interfacial assembly of protein-polymer nano-conjugates into stimulus-responsive biomimetic protocells, *Nature Commun.* 4 (2013) 2239.

[68] X. Huang, A.J. Patil, M. Li, S. Mann, Design and construction of higher-order structure and function in proteinosome-based protocells, *J. Am. Chem. Soc.* 136 (2014) 9225-9234.

[69] P. Zhou, X. Liu, G. Wu, P. Wen, L. Wang, Y. Huang, X. Huang, Programmable modulation of membrane permeability of proteinosome upon multiple stimuli responses, *ACS Macro Lett.* 6 (2017) 689-694.

[70] D. Su, J. Qi, X. Liu, L. Wang, H. Zhang, H. Xie, X. Huang, Enzyme-modulated anaerobic encapsulation of chlorella cells allows switching from O<sub>2</sub> to H<sub>2</sub> production. *Angew. Chem., Int. Ed.* 58 (2019) 3992-3995.

